2003

Novel Examples of Achiral Bent-Core Azo Compounds Exhibiting B1 and Anticlinic-Antiferroelectric B2 Mesophases

Veena Prasad
Shin-Woong Kang, *Kent State University - Kent Campus*
Satyendra Kumar, *Kent State University*

JOURNAL OF Materials CHEMISTRY

Novel examples of achiral bent-core azo compounds exhibiting B_1 and anticlinic–antiferroelectric B_2 mesophases

Veena Prasad,[a] Shin-Woong Kang[b] and Satyendra Kumar*[b]

[a]*Center for Liquid Crystal Research, P. B. No. 1329, Jalahalli, Bangalore 560013, India*
[b]*Department of Physics, Kent State University, Kent, OH 44242, USA.*
E-mail: satyen@xray.kent.edu

Received 21st February 2003, Accepted 4th April 2003
First published as an Advance Article on the web 23rd April 2003

The first examples of achiral bent-core molecules consisting of an azo linkage and five aromatic rings exhibiting bent-core mesophases are reported. They exhibit B_1 and B_2 phases as identified by optical microscopy, differential scanning calorimetry, X-ray diffraction, and electro-optical techniques. The B_2 phase of these materials is identified to be the anticlinic–antiferroelectric, SmC_AP_A phase. The mesophases of these compounds have relatively low transition temperatures and wide temperature ranges. The observation of bent-core phases in azo compounds assumes significance from the fact that the introduction of the –N=N– linkage adds a new dimension, namely photochromism, to this field.

Introduction

Ferro- and antiferroelectric liquid crystalline compounds composed of bent-shaped achiral molecules are very interesting subjects which have recently attracted much attention. Since the discovery[1] of such materials exhibiting new types of mesophases, various structural variants of the parent compound, *i.e.*, 1,3-phenylene bis[4-(4-n-alkylphenyliminomethyl)-benzoates], have been reported.[2–6] Up to now, at least seven different mesophases, B_1–B_7, have been identified and characterized[4] in compounds with bent-core molecules. The B_2 phase has been studied in depth by Walba and Clark.[7,8] They have shown the formation of four different variants of the B_2 phase differing in their molecular tilt and ferroelectricity. Some of the phases are found to be electro-optically switchable. The B_1 phase formed by such compounds has recently been designated as a rectangular columnar mesophase.[5]

A literature survey of liquid crystals composed of bent-shaped molecules reveals that compounds with azo linkages have remained unexplored. From the view point of chemical structure, bent-core molecules with five, six and seven aromatic rings have been found to form liquid crystal phases. However, no compounds consisting of an azo linkage have so far been reported to form bent-core mesophases. The observation of bent-core phases in azo compounds is significant because of their photochromic properties as the –N=N– linkage undergoes *trans–cis* isomerization in the presence of UV light. Towards this end, the first compound which we synthesized[9] was 1,3-phenylene bis[4-(4′-decyloxyphenylazo)benzoate], but it did not exhibit mesomorphism. Therefore, an imino linkage was introduced in this molecule, as it has been found that the –CH=N– linkage is more conducive to mesomorphism. As expected, this material formed bent-core mesophases.[10] Several structural variants of this compound were subsequently synthesized and found to form different types of bent-core mesophases.[11] But, due to their high transition temperatures we could not carry out a detailed characterization and phase identification. Since then, efforts have been focussed on lowering the transition temperatures so that they are better suited for easy physical characterization. Thus, compounds with highly unsymmetric bent-shaped molecules consisting of an azo linkage and five aromatic rings were designed and synthesized. The molecular structure of these ten new compounds is shown in Fig. 1. With this modification, the transition temperatures were drastically lowered without losing their mesomorphic properties. All these compounds have been found to be thermally stable and suitable for the physical studies.

The molecule is said to be symmetric with respect to the linkage groups, when **X** is the same as **X′** and **Y** is the same as **Y′** (*e.g.*, X: –COO–, Y: –N=N–, **X′**: –CH=N–, and **Y′**: –COO– in Fig. 1). The molecule is unsymmetric when the linking group **X** differs from **X′** or **Y** differs from **Y′**. Unsymmetric bent-core liquid crystalline compounds wherein **X** differs from **X′** have been reported in the literature.[4] But, no such examples are known wherein **Y** also differs from **Y′**. In fact, we had previously synthesized a compound of this type, in which a –CH=N– linkage was used in the place of –N=N– (in structures **5a–e**), *i.e.*, the two types of linkages –CH=N– and –COO– were alternatively used to bridge the five aromatic rings to each other to form a bent-core molecule. But this compound was found to be non-liquid crystalline. Therefore, it appears that the existence of bent-core mesophases depends not only on the shape of the molecules but also on other parameters, such as local dipolar moments, positions of different charges and the extent of conjugation, *etc*. Now, in the present molecular structures (**4a–e** and **5a–e**), both linkage groups **X** and **Y** in one arm differ from the linkages **X′** and **Y′** on the other arm of the molecule, respectively. Evidently, this molecule is highly unsymmetric. To the best of our knowledge, synthesis of such unsymmetric bent-shaped molecules consisting of five aromatic rings with three different types of linkage units (–COO–, –CH=N– and –N=N–) bridging the aromatic rings to each other has not been reported before.

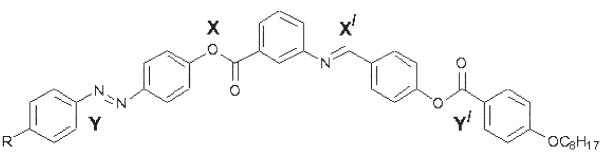

4a-e: R = C_4H_9, C_6H_{13}, C_8H_{17}, $C_{10}H_{21}$, $C_{12}H_{25}$

5a-e: R = OC_4H_9, OC_6H_{13}, OC_8H_{17}, $OC_{10}H_{21}$, $OC_{12}H_{25}$

Fig. 1 Molecular structure of the ten new azo compounds synthesized shown with different substituent groups.

DOI: 10.1039/b302018e

Experimental

Synthesis

AR quality chemicals and solvents were obtained locally and used without further purification. However, the solvents were dried using standard methods, wherever required. The purity and the chemical structures of all the ten compounds synthesized were confirmed by spectral data. ^{1}H NMR spectra were recorded in $CDCl_3$, on a 200 MHz Bruker Aveance Series DPX-200 NMR spectrometer, using Me_4Si as an internal standard. Microanalyses were performed using a Eurovector Elemental Analyzer, Model Euro EA 3000.

The synthesis of these novel azo compounds was achieved by following the routes shown in Fig. 2. The synthesis methods used in this scheme are classical. The aldehyde **1**, obtained by the esterification of 4-hydroxybenzaldehyde and 4-n-octyloxybenzoic acid, was reacted with 3-aminobenzoic acid in ethyl alcohol under refluxing conditions, to get the acid **2**, which was purified by recrystallization twice, using ethyl alcohol. All the required 4-n-alkyl/alkyloxy-4′-hydroxyazobenzenes **3** were prepared following a procedure reported previously.[12] Finally, the acid **2** was esterified with the hydroxy compound **3**, in the presence of 1,3-dicyclohexylcarbodiimide (DCC) and dimethylaminopyridine (DMAP) as catalyst using dry dichloromethane as solvent. The final liquid crystalline compounds **4a–e** and **5a–e** thus obtained were purified by several recrystallisations using butan-2-one as the solvent. The spectral data and the microanalyses obtained for all the compounds were satisfactory. The analytical data for the intermediate compounds **1** and **2** and for one of the representative compounds from each series **4a–e** and **5a–e** are given below.

Compound 1. Cr 55.5 °C N 65.0 °C I. IR ν_{max}/cm^{-1} (KBr pellet): 2910, 2847, 1734, 1701, 1605, 1578, 1512, 1468, 1422, 1385, 1267, 1215, 1169, 1071, 1011, 882, 845. ^{1}H NMR ($CDCl_3$) δ: 10.02 (s, 1H, –CHO), 8.14 (d, 2H, ArH), 7.97(d, 2H, ArH), 7.40 (d, 2H, ArH), 6.98 (d, 2H, ArH), 4.05 (t, 2H, Ar–OCH_2–), 1.31–1,86 (m, 12H, –CH_2–), 0.88 (t, 3H, –CH_3). Elemental anal.: calcd. for $C_{22}H_{26}O_4$, C, 74.55, H, 7.39: found, C, 74.49, H, 7.5%.

Compound 2. M.p. 164 °C. IR ν_{max}/cm^{-1} (KBr pellet): 3440, 2922, 2851, 1726, 1681, 1606, 1578, 1509, 1453, 1288, 1253, 1201, 1170, 1086, 849. ^{1}H NMR ($CDCl_3$) δ: 8.52 (s, 1H, –CH=N–), 8.15 (d, 2H, ArH), 7.97 (m, 4H, ArH), 7.33–7.56 (m, 4H, ArH), 6.96 (d, 2H, ArH), 4.05 (t, 2H, Ar–OCH_2–), 1.32–1.86 (m, 12H, –CH_2–), 0.87 (t, 3H, –CH_3). Elemental anal.: calcd. for $C_{29}H_{31}NO_5$, C, 73.55, H, 6.60, N, 2.96: found, C, 73.59, H, 6.7, N, 2.87%.

Compound 4e. IR ν_{max}/cm^{-1} (KBr pellet): 2920, 2851, 1731, 1598, 1509, 1468, 1273, 1231, 1205, 1169, 1076, 845. ^{1}H NMR ($CDCl_3$) δ: 8.55 (s, 1H, –CH=N–), 6.96–8.19 (m, 20H, ArH), 4.05 (t, 2H, Ar–OCH_2–), 2.69 (t, 2H, Ar–CH_2–), 1.26–1.86 (m, 32H, –CH_2–), 0.88 (m, 6H, –CH_3). ^{13}C NMR (100 MHz, $CDCl_3$) δ: 164.6, 163.8, 160.3, 153.9, 152.7, 152.4, 150.9, 150.5, 146.7, 133.4, 132.3, 130.5, 130.2, 129.5, 129.1, 127.6, 126.7, 124.0, 122.9, 122.4, 122.3, 122.1, 121.2, 114.4, 68.4, 35.9, 31.9, 31.8, 31.2, 29.6, 29.5, 29.3, 29.2, 29.1, 26.0, 22.6, 14.0. Elemental anal.: calcd. for $C_{53}H_{63}N_3O_5$, C, 77.43, H, 7.72, N, 5.11: found, C, 77.29, H, 7.93, N, 5.13%.

Compound 5e. IR ν_{max}/cm^{-1} (KBr pellet): 2919, 2850, 1738, 1603, 1509, 1469, 1283, 1252, 1232, 1171, 1081, 840. ^{1}H NMR ($CDCl_3$) δ: 8.55 (s, 1H, –CH=N–), 6.95–8.17 (m, 20H, ArH), 4.05 (t, 4H, Ar–OCH_2–), 1.27–1.86 (m, 32H, –CH_2–), 0.88 (m, 6H, –CH_3). ^{13}C NMR (100 MHz, $CDCl_3$) δ: 164.7, 163.8, 161.8, 160.3, 153.9, 152.4, 150.6, 146.9, 133.5, 132.3, 130.5, 130.2, 129.5, 127.6, 126.7, 124.8, 123.7, 122.3, 122.2, 122.0, 121.3, 114.8, 114.4, 68.4, 31.9, 31.8, 29.5, 29.3, 29.2, 29.1, 26.0, 22.6, 14.0. Elemental anal.: calcd. for $C_{53}H_{63}N_3O_6$, C, 75.96, H, 7.58, N, 5.01: found, C, 75.92, H, 7.63, N, 5.09%.

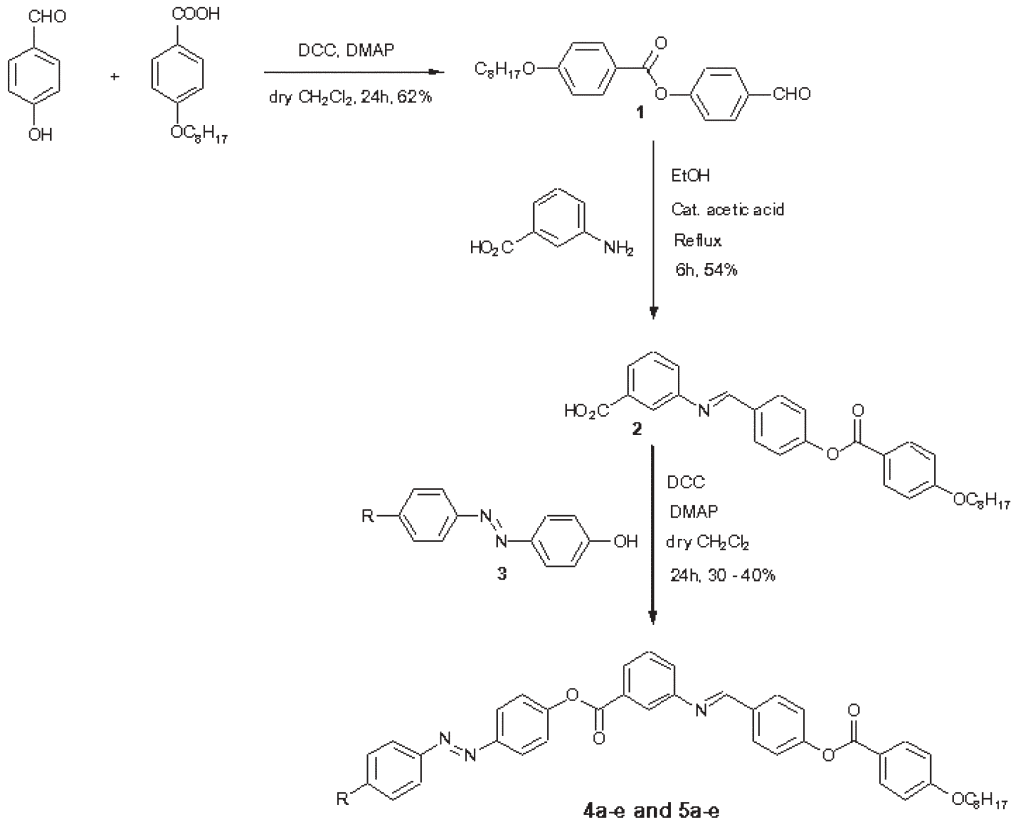

Fig. 2 The synthesis scheme followed for the synthesis of azo compounds.

Mesophase characterization

The microscopic textural observations were carried out using a Mettler FP82HT hot stage in conjunction with a Leitz DMRXP polarizing microscope. The exact transition temperatures of different phase transitions and the associated enthalpies were determined from differential scanning calorimetric scans (DSC7, Perkin-Elmer). The heating and cooling rates were 5 °C min^{-1}.

The compounds **4e**, **5e**, and **5c** were selected for physical characterization of their phase behavior by X-ray scattering and electro-optical techniques due to their relatively low transition temperatures.

X-Ray studies were carried out at the Advanced Photon Source of Argonne National Laboratory using the Midwestern Universities Collaborative Team's beamline on Sector 6. The samples were sealed in 1 mm diameter Lindeman capillaries and aligned in the presence of a magnetic field of ~2.5 kG by cooling to mesophase temperatures from the isotropic melt. Sample temperature was controllable with a precision of ±0.1 °C using a home made oven and temperature controller. A wavelength of 0.7653 Å was used. The diffraction patterns were collected using a high-resolution MAR3450 area detector placed at a distance of 586.62 mm from the sample. The 2θ scans were generated from the 2-D diffraction patterns using the software package FIT2D developed by A. P. Hammersley of the European Synchrotron Radiation Facility.

For electro-optical studies, the sample was sealed in flat glass cells of 2 μm thickness. Glass plates with ITO layer and polyimide alignment layers were assembled with antiparallel rubbing directions. The electro-optical response was studied by applying different waveforms of the applied voltage. Spontaneous polarization, P, was measured using a triangular waveform of 10 Hz and a peak voltage, V_p, ranging from 0 to 80 V. The applied signal and current through the sample were recorded using a Tektronix oscilloscope model TDS-340A.

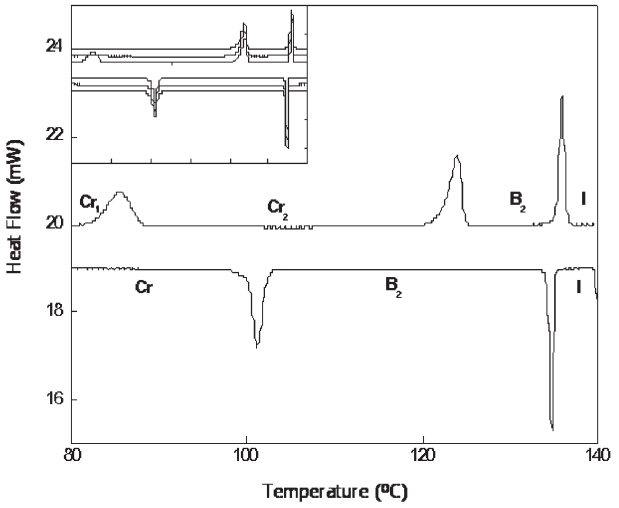

Fig. 3 DSC thermograms for compound **4e**. The heating/cooling rate was 5 °C min^{-1}. The inset shows the reproducibility of the transition temperatures on three consecutive heating and cooling cycles. Note that all the three heating and cooling scans are perfectly overlapping, thus showing the thermal stability of the compound.

Results and discussion

The mesomorphism of all the compounds was investigated using polarizing microscope and differential scanning calorimetry. The DSC scans of each of these compounds were run several times by raising their temperatures well above the clearing point. The thermal behavior was found to be reproducible and all of the compounds thermally very stable. A representative set of thermograms, the DSC scans of sample **4e**, are shown in Fig. 3. The inset shows the first and subsequent heating and cooling scans. The transition temperatures and associated transition enthalpies obtained from the DSC thermograms are summarized in Table 1. The peak temperatures are given in °C and the numbers in the parentheses indicate the transition enthalpy (ΔH) in kJ mol^{-1}. As can be seen from Table 1, all the ten compounds synthesized are found to be liquid crystalline. In both **4a–e** and **5a–e** series, all compounds are found to form the B_1 phase, except for the highest homologues (R = $C_{12}H_{25}$ and $OC_{12}H_{25}$) which form the B_2 phase. In compounds **4a–e**, the lower homologues are monotropic whereas the higher ones are enantiotropic. However, all the compounds **5a–e** are found to be enantiotropic.

In the present study, the chain length at one end was fixed to be OC_8H_{17} and the chain length (R) at the other end of the molecule was systematically changed. Again, R was chosen to be one of the two types of substitutions, alkyl (**4a–e**) or alkoxy (**5a–e**) chains. The nature of the substitution R, *i.e.*, whether alkyl or alkoxy, did not affect the nature of the mesophase exhibited. However, the compounds with alkyl chains (**4a–e**) were found to have considerably lower transition temperatures than those with alkoxy chains (**5a–e**). Almost all the compounds exhibited one or more crystal–crystal transitions before melting. In some cases, it was also found that the solvent crystallized and the melt-crystallized solids had different melting points, most likely due to different crystal structures. The mesophase ranges were found to be wider for alkoxy compounds (**5a–e**) than the corresponding alkyl chain compounds (**4a–e**). The melting points as well the clearing temperatures decreased as the chain length of R increased.

Optical microscopy textures of samples **4e** and **5c** are shown in Fig. 4. On cooling from the isotropic phase, compound **4e** exhibits spherulitic domains with a fringe pattern. The schlieren texture can also be seen in some regions. This is a typical texture observed for the B_2 mesophase.[13] Similar optical textural behaviour was observed for compound **5e** as well. On cooling from the isotropic phase, compound **5c** forms batonnets along with some rectangular domains [Fig. 4(b)]

Table 1 Transition temperatures and enthalpies of the compounds synthesized

Compound	R	1st Heating scan	1st Cooling scan
4a	C_4H_9	Cr 145.8 (34.5) I	I 137.0 B_1[a] 136.1 (35.9) Cr
4b	C_6H_{13}	Cr 142.1 (35.1) I	I 140.8 (15.4) B_1 126.0 (16.9) Cr
4c	C_8H_{17}	Cr 140.5 (36.7) I	I 139.3 (15.8) B_1 128.1 (19.3) Cr
4d	$C_{10}H_{21}$	Cr 131.0 (15.9) B_1 136.4 (12.7) I	I 134.6 (12.6) B_1 114.4 (15.2) Cr
4e	$C_{12}H_{25}$	Cr 124.0 (23.4) B_2 135.9 (18.4) I	I 134.7 (18.4) B_2 101.2 (20.1) Cr
5a	OC_4H_9	Cr 151.3 (19.4) B_1 158.4 (17.0) I	I 157.5 (16.4) B_1 145.0 (17.4) Cr
5b	OC_6H_{13}	Cr 146.9 (25.8) B_1 157.2 (22.9) I	I 155.9 (16.4) B_1 136.1 (15.7) Cr
5c	OC_8H_{17}	Cr 138.6 (21.0) B_1 153.4 (18.2) I	I 151.8 (19.0) B_1 132.2 (19.5) Cr
5d	$OC_{10}H_{21}$	Cr 134.5 (22.3) B_1 147.0 (181.1) I	I 145.7 (180.0) B_1 126.6 (21.2) Cr
5e	$OC_{12}H_{25}$	Cr 125.4 (58.8) B_2 142.8 (20.0) I	I 141.7 (19.8) B_2 107.7 (19.4) Cr

[a]Enthalpy could not be measured due to the onset of crystallization.

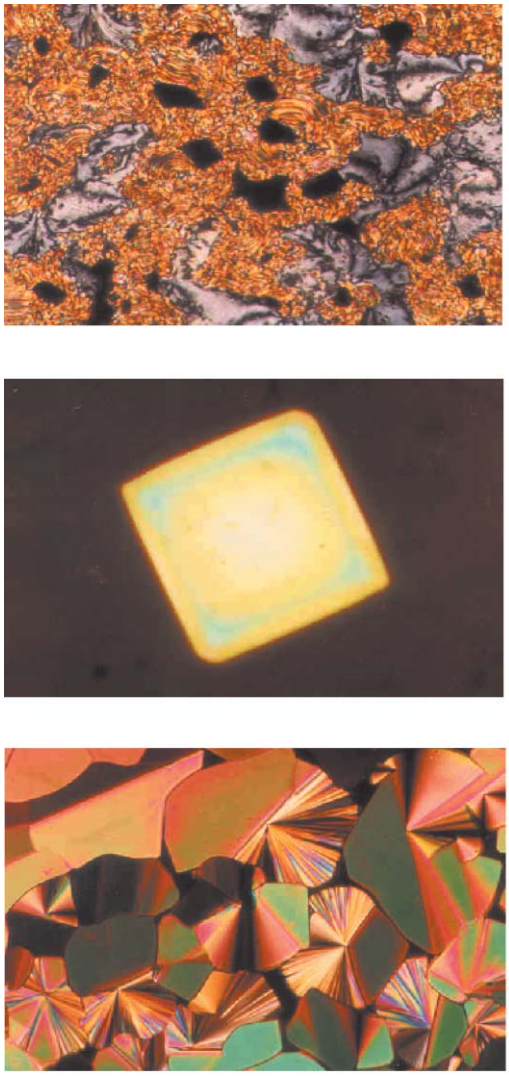

Fig. 4 Optical polarizing microscopy textures of the two types of compounds synthesized. (a) The spherulitic domains with fringe patterns of the B_2 phase exhibited by compound **4e** at 132 °C. In some regions schlieren texture is also seen. (b) The rectangular domain pattern of the B_1 phase growing from the isotropic liquid of compound **5c**, at 152 °C. On further cooling, the typical mosaic texture observed for the B_1 phase of compound **5c**, at 148 °C, is shown in (c).

which coalesce into a mosaic texture [Fig. 4(c)]. This is a characteristic feature of the bent-core mesophase B_1, which has recently been designated as a rectangular columnar mesophase.[5] The same type of textural behaviour was observed for all the other compounds exhibiting a B_1 phase and listed in Table 1.

The X-ray diffraction patterns for different compounds were recorded upon cooling from the isotropic phase. The samples were cycled several times through the clearing point in the presence of the magnetic field to align them. But, in practically all cases, we invariably obtained powder diffraction patterns because the external applied magnetic field was unable to orient the director and align the LC phase in these materials without the nematic phase.

Sample **4e** exhibited a single domain diffraction pattern when it was crystallized from the liquid crystalline phase. The alignment persisted when it was heated back to the liquid crystalline phase. The two dimensional single domain diffraction pattern for the LC phase of compound **4e** at 132.9 °C is shown in Fig. 5. This pattern is very similar to that previously reported for a single domain B_2 phase.[4,14] It is clear from the diffraction pattern that two orders of smectic layer reflections are visible corresponding to $2\theta = 1.17$ and 2.34°. The intensity

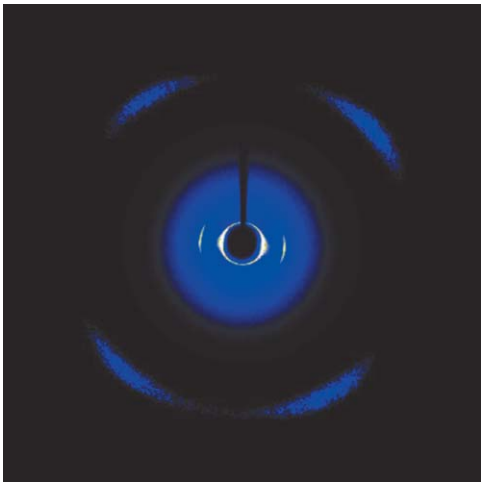

Fig. 5 X-Ray diffraction pattern of a single domain B_2 phase of **4e**. The angle between the directions of the small and large angle reflections yields the molecular tilt angle to be $37 \pm 2°$.

of the first peak was much higher than the second. From the diffraction pattern, the molecular tilt angle with respect to the smectic layer normal was estimated from the angle between the small angle smectic layer reflections and the large angle reflections from the intermolecular distance. It is clear from the four symmetric large angle peaks that the molecules are tilted at $37 \pm 2°$ to either side of the layer normal with equal probability indicating an anticlinic arrangement in an SmC like phase.

The powder diffraction patterns for samples **5e** (at 140.5 °C) and **5c** (at 142.2 °C) are shown in Figs. 6 and 7, respectively. In the cases of these two compounds, it was not possible to obtain single domains. The 2θ scans generated from the diffraction patterns are shown in Fig. 8 for all three compounds. From a comparison of the relative positions and intensities of the three peaks for **4e** and **5e** it can be safely concluded that these compounds have the same LC phase, namely the B_2 phase. On the other hand, the diffraction pattern of compound **5c** has two bright peaks at small angles. In contrast to the diffraction of the B_2 phase, the intensity of the second peak is much higher than the first peak. It resembles a previously reported[10] diffraction pattern for the B_1 phase. Thus the results of X-ray diffraction experiment confirm the preliminary phase identification made on the basis of optical textures. The diffraction angles and layer spacings corresponding to the peaks observed for these compounds are summarized in Table 2.

Electro-optical characteristics of these materials were studied in the middle of the LC phases. Sample **4e** was found to be very responsive to applied fields. Its response to applied triangular

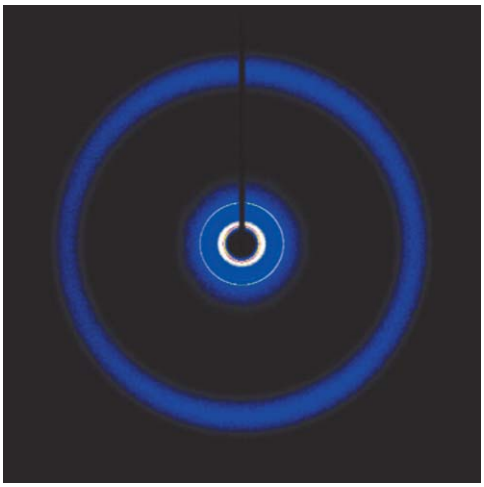

Fig. 6 Powder X-ray diffraction pattern of the B_2 phase of **5e**.

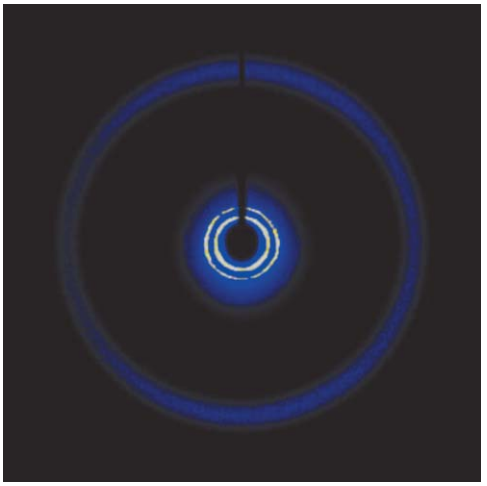

Fig. 7 Powder diffraction pattern of the B_1 phase of compound **5c**.

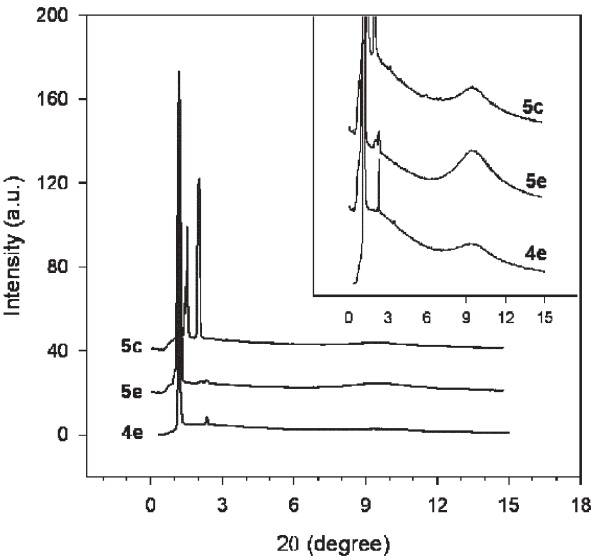

Fig. 8 Powder X-ray diffractographs of samples **4e**, **5c** and **5e**.

wave voltage signal of 10 Hz measured at 120 °C is shown in Fig. 9. The solid curve was obtained for V_p = 80 V and open circles for V_p = 50 V. It is clear from the double polarization reversal peaks[4,15] that this is an antiferroelectric phase. The values of spontaneous polarization P varied somewhat with the applied voltage from 587 nC cm^{-2} for V_p = 50 V to 703 nC cm^{-2} for V_p = 80 V. When these results are interpreted in light of the X-ray results discussed above, we conclude that this is a B_2, or more precisely, the anticlinic–antiferroelectric SmC_AP_A, phase.

To study the electro-optical properties of this compound, a cell filled with compound **4e** was placed between a polarizer

Table 2 Peak positions in 2θ and lattice spacings in Å obtained from X-ray diffraction for the three compounds **4e**, **5e**, and **5c**

Sample	Peak no.	2θ/°	Spacing/Å
5c	1	1.52	28.93
	2	1.99	22.02
	3	9.49	4.63
5e	1	1.17	37.38
	2	2.32	18.92
	3	9.64	4.55
4e	1	1.18	37.24
	2	2.34	18.76
	3	9.38	4.68

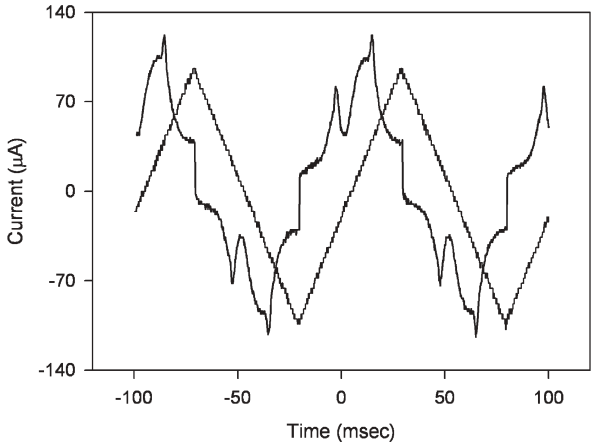

Fig. 9 Current *vs.* time and the applied triangular signal applied across a cell to measure the spontaneous polarization of compound **4e**.

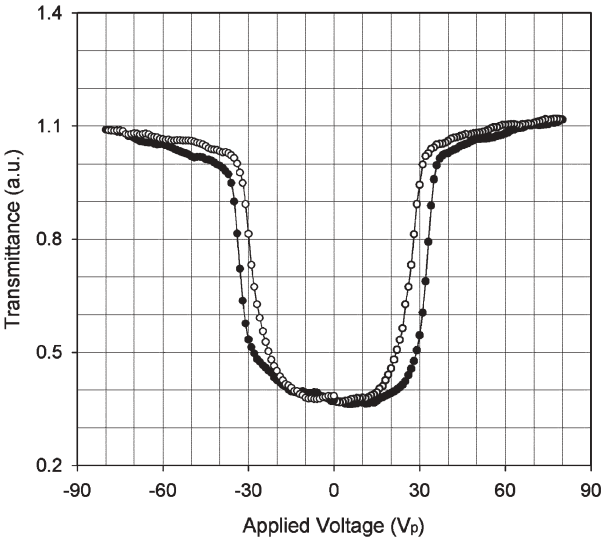

Fig. 10 Transmission *vs.* applied voltage across a LC cell filled with **4e** whose hysteresis establishes the antiferroelectric nature of this phase; solid line for V_p = 80 V and open circles for V_p = 50 V.

and a crossed analyzer and its orientation adjusted to give minimum transmission in the absence of applied field. Then, the transmitted intensity of light was measured as a function of applied ac voltage of frequency 1 Hz. The hysteretic behavior shown in Fig. 10 was obtained in the liquid crystalline phase at 120 °C. Here, filled circles indicate a field-induced transition to ferroelectric states. Open circles represent relaxation back to the antiferroelectric state. Stripe domains appear in the presence of high field in the ferroelectric state. These changes in the optical textural are very similar to those described in references 4, 12–16.

Compound **5e** showed a weak response to applied electric field. We believe that this may be due to the higher viscosity and lower P for this compound. These observations are in agreement with the inferences drawn about the nature of the LC phase (*i.e.*, B_2) of this compound. Sample **5c** did not exhibit any electrical response leading us to believe that it is neither a ferro nor antiferroelectric phase, as expected from a B_1 phase.

Conclusions

In summary, we have reported the synthesis and mesomorphic properties of highly unsymmetric bent-core azo compounds containing five aromatic rings. Optical polarizing microscopy,

high-resolution synchrotron X-ray diffraction studies, and electro-optical methods reveal the nature and structure of their liquid crystalline phases to be anticlinic–antiferroelectric SmC_AP_A (or antiferroelectric B_2) and B_1 phases. These photochromic and electrically responsive materials should find novel technological uses. Investigations on various structural variants of these azo compounds **4a–e** and **5a–e** are presently in progress.

Acknowledgements

Funding for this work was provided, in part, by the Ohio Board of Regents under its Research Challenge program. Use of the Advanced Photon Source (APS) was supported by the U.S. Department of Energy, Basic Energy Sciences, Office of Science, under Contract No. W-31-109-Eng-38. The Midwest Universities Collaborative Access Team (MUCAT) sector at the APS is supported by the U.S. Department of Energy, Basic Energy Sciences, Office of Science, through the Ames Laboratory under Contract No. W-7405-Eng-82.

References

1 T. Niori, T. Sekine, J. Watanabe, T. Furukava and H. Takezoe, *J. Mater. Chem.*, 1996, **6**, 1231.
2 D. Shen, S. Diele, I. Wirth and C. Tschierske, *Chem. Commun.*, 1998, 2573.
3 D. Shen, S. Diele, G. Pelzl, I. Wirth and C. Tschierske, *J. Mater. Chem.*, 1999, **9**, 661.
4 G. Pelzl, S. Diele and W. Weissflog, *Adv. Mater.*, 1999, **11**, 707 and references therein.
5 D. Shen, A. Pegenau, S. Diele, I. Wirth and C. Tschierske, *J. Am. Chem., Soc.*, 2000, **122**, 1593; J. Watanabe, T. Niori, T. Sekine and H. Takezoe, *Jpn. J. Appl. Phys.*, 1998, **37**, L139.
6 J. C. Rouillon, J. P. Marcerou, M. Laguerre, H. T. Nguyen and M. F. Achard, *J. Mater. Chem.*, 2001, **11**, 2946.
7 D. M. Walba, E. Korblova, R. Shao, J. E. Maclennan, D. R. Link, M. A Glaser and N. A. Clark, *Science*, 2000, **288**, 2181.
8 D. R. Link, G. Natale, R. Shao, J. E. Maclennan, E. Korblova and D. M. Walba, *Science*, 1997, **278**, 1924.
9 V. Prasad, *Liq. Cryst.*, 2001, **28**, 145.
10 V. Prasad, D. S. S. Rao and S. K. Prasad, *Liq. Cryst.*, 2001, **28**, 643.
11 V. Prasad, *Mol. Cryst. Liq. Cryst.*, 2001, **363**, 167.
12 T. Ikeda, T. Miyamoto, S. Kurihara, M. Tsukada and S. Tazuke, *Mol. Cryst. Liq. Cryst.*, 1990, **182B**, 357.
13 T. Sekine, T. Niori, M. Sone, J. Watanabe, S. W. Choi, Y. Takanishi and H. Takezoe, *Jpn. J. Appl. Phys.*, 1997, **36**, 6455.
14 G. Pelzl, S. Diele, S. Grande, A. Jakli, C. Lischka, H. Kresse, H. Schmalfuss, I. Wirth and W. Weissflog, *Liq. Cryst.*, 1999, **26**, 401.
15 H. Kresse, S. Schlacken, U. Dunemann, M. W. Schroder, G. Pelzl and W. Weissflog, *Liq. Cryst.*, 2002, **29**, 1509.
16 S. V. Shilov, S. Rauch, H. Skupin, G. Heppke and F. Kremer, *Liq. Cryst.*, 1999, **26**, 1409.